

Oral soft tissue laser ablative and coagulative efficiencies spectra

Dr. Peter Vitruk delves into the science behind ablative soft tissue lasers

Introduction

The much praised clinical benefits and ease of use of surgical and dental lasers are enjoyed by millions of patients and by tens of thousands of physicians, dentists, and veterinarians worldwide. State-of-the-art modern-day soft tissue lasers have made many soft tissue procedures much simpler and far more enjoyable for practitioners — consider bloodless laser blepharoplasty and laser frenectomy in Figures 1 and 2.

The key to the success of soft tissue lasers is their ability to cut and coagulate the soft tissue at the same time. Present work is aimed to derive the wavelength-dependent differences in photo-thermal ablation and coagulation efficiencies for oral soft tissue pulsed dental Near-IR Diode, Mid-IR Erbium and IR CO₂ lasers.¹⁻²⁴

Even though the soft tissue photo-thermal ablation has been extensively studied,^{5,6,17} there remains a discrepancy between (a) the widely proliferated notion about efficient Near-IR 800-1,100 nm laser ablation of the oral soft tissue,^{25,26} and (b) studies reporting the inefficient soft tissue Near-IR absorption/ablation.^{5,6,17,18}

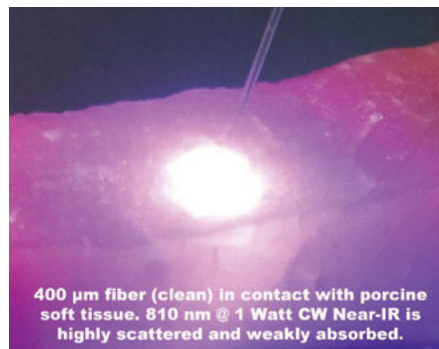
Indeed, the notions about “the key to the usefulness of the Nd:YAG is that this wavelength is highly absorbed in oral soft tissue”²⁵, and “all currently available dental laser instruments and their emission wavelengths have indications for use for incising, excising ... oral soft tissue surgery”²⁶, contradict an observation⁵ illustrated here by Figure 3: “Lasers whose extinction length



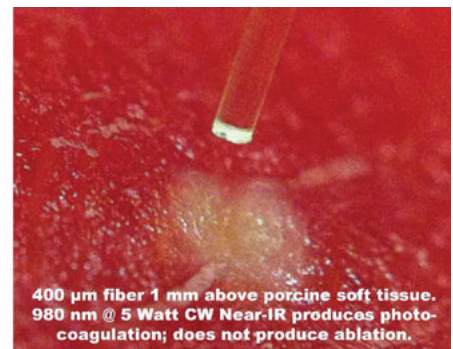
Figure 1: CO₂ laser blepharoplasty in progress
(Photo courtesy of Edward M. Zimmerman, MD, Pres. American Board of Laser Surgery, Las Vegas, Nevada)



Figure 2: CO₂ laser frenectomy in progress
(Photo courtesy of Alan Winner, DDS, New York, New York)



400 μm fiber (clean) in contact with porcine soft tissue. 810 nm @ 1 Watt CW Near-IR is highly scattered and weakly absorbed.



400 μm fiber 1 mm above porcine soft tissue. 980 nm @ 5 Watt CW Near-IR produces photo-coagulation; does not produce ablation.

Figure 3: Near-IR wavelengths 810 and 980 nm from commercially available dental diode lasers are highly scattered and weakly absorbed by the porcine soft tissue, resulting in slow and widespread photo-coagulation and no ablation

is 5 mm or more, and whose δ/α ratio [scattering to absorption ratio] is larger than 10, make good coagulators but poor scalpels. Such wavelengths are all in the near-infrared (700-1400 nm) region.”

Another review article¹⁷ reports that “Using laser wavelengths where optical scattering is comparable to or dominant over tissue absorption is not conducive to precise ablation” directly relates to Near-IR wavelengths 800-1,100 nm.

Furthermore, “Even in an idealized situation, application of high power laser [810 nm] light (e.g., 20 W) is necessary during several seconds, inducing tissue changes that extend further into the tissue than can be observed by the surgeon. An important complicating factor in the use of this high-power laser light, which penetrates deeply before being absorbed totally, is that it may

reach vital structures in the vicinity of the target tissue. These vital structures ... may preferentially absorb near-infrared laser light because of different optical properties and may be heavily damaged before efficient tissue ablation at the surface initiated.”¹⁸

To address the preceding discrepancies, present work utilizes the known optical absorption coefficient spectra of the oral soft tissue’s four main chromophores — water,^{1,2} melanin,^{3,4} hemoglobin (Hb), and oxyhemoglobin (HbO₂)⁴⁻⁶ (see Figure 4) — in order to analyze the photo-thermal ablation (or photovaporolysis⁵) and photo-thermal coagulation (or photopyrolysis⁵) efficiencies for the soft tissue dental lasers⁷ on the market today: Near-IR diodes at 808 - 1,064 nm; Mid-IR Erbium lasers at 2,780 nm and 2,940 nm; and IR CO₂ laser at 9,300 nm and 10,600 nm.



Prior to co-founding LuxarCare in 2002 and LightScalpel in 2005, Peter Vitruk, PhD, MInstP, CPhys, held a variety of research and development positions around the globe. He was a Research Scientist with The Academy of Sciences in the former USSR and a Visiting Research Fellow with Heriot-Watt University in Edinburgh, United Kingdom (UK). He later worked as RF-excited CO₂ Laser Programs Manager with Synrad, Inc., and then as Chief Scientist/Laser Designer with Luxar/ESC/Lumenis. He has authored 10 patents and over 20 articles on RF-excited CO₂ gas laser plasma and resonator technology and is a Member of The Institute of Physics, London, UK. Author can be contacted at pvitruk@lightscalpel.com.

Optical model for epithelium and connective tissue (sub-epithelium)

Besides the absorption coefficient spectra for the soft tissue's main chromophores, their respective spatial distributions are taken into account through a simple two-layer optical model depicted in Figure 5:

- The 100-300 μm thin⁸ epithelium layer with its optical absorption dominated by melanin and water.
- The sub-epithelium medium (connective tissue, inclusive of lamina propria and submucosa^{9,10}) with its optical absorption dominated by water and hemoglobin/oxyhemoglobin.

75% water content is assumed for both epithelium and sub-epithelium for convenience; adjusting water content within 70-100% range does not significantly alter main results and conclusions of this study.

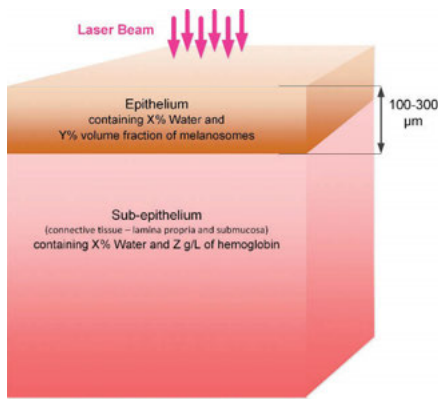


Figure 5: Simplified optical model of oral soft tissue consisting of (1) water-melanin rich epithelium layer, and (2) water-hemoglobin-oxyhemoglobin rich sub-epithelium medium (connective tissue inclusive of lamina propria and submucosa)

Photo-thermal laser-tissue interaction: absorption, ablation, coagulation

During photo-thermal laser-tissue interaction, the laser beam energy is absorbed (by tissue's main chromophores-absorption centers) and heats the tissue inside the irradiated volume, which leads to elevated tissue temperatures that can result in tissue ablation and coagulation.

Consider, as shown in Figure 6, a one-dimensional approximation of a laser beam irradiating the tissue surface (at $x=0$) from the left (is graphically represented as a thin slice of a laser beam directed at the thin slice of the tissue), assuming pulse duration is essentially shorter than Thermal Relaxation Time discussed later. Incident laser beam

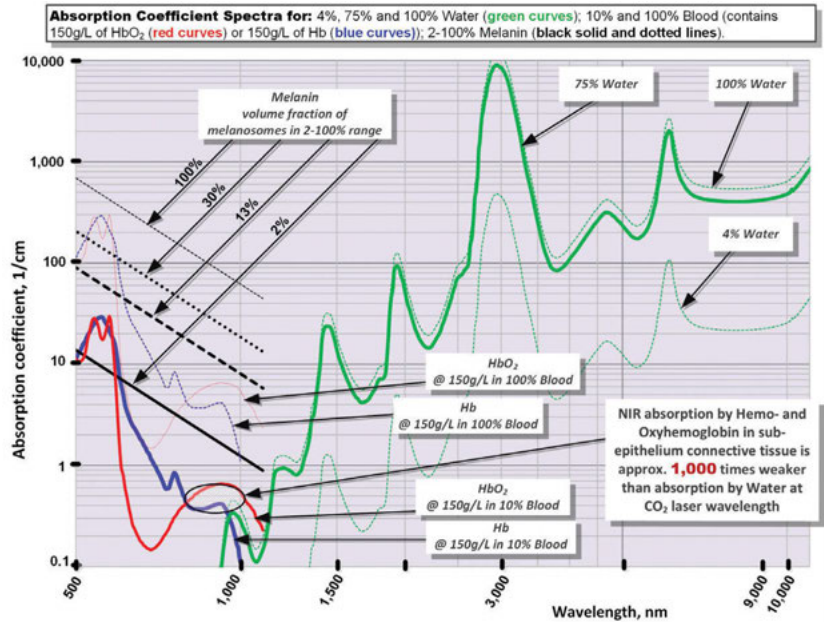


Figure 4: Optical absorption coefficient spectra at different histologically relevant concentrations of water, hemoglobin, oxyhemoglobin, and melanin based on data from references 1-6. Logarithmic scales are in use

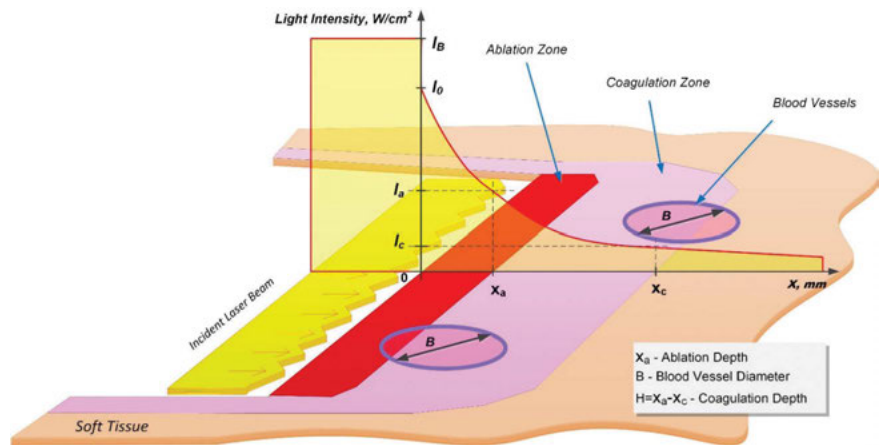


Figure 6: Simplified graphical representation of laser beam intensity attenuated inside the soft tissue

intensity $[W/cm^2]$ is I_B ; laser light intensity immediately below the tissue surface is I_0 . Accordingly, the reflectivity of tissue' surface is $(I_B - I_0)/I_B$, and the transmission is I_0/I_B . Inside the tissue, i.e., for $x > 0$, the laser light intensity is exponentially attenuated:

$$I = I_0 \text{Exp} [-x/A] \tag{1}$$

where $1/A$ is absorption coefficient from Figure 4 (or attenuation coefficient if light scattering is taken into account). Assuming that laser intensity I_0 is greater than intensity I_a required (for a specific pulse duration t) to ablate the tissue locally, the tissue ablation takes place in $0 < x < x_a$ referred to as the "ablation zone" in Figure 6. Immediately below the ablation zone the heat affected zone $x_a < x < x_c$ is located, with the tissue

temperature ranging from the very high T_a (ablation temperature) at x_a all the way down to the coagulation threshold temperature T_c at x_c (i.e., $T_a = 100^\circ\text{C}$ and $T_c = 60^\circ\text{C}$). Coagulation depth $H = x_c - x_a$ is defined by 60-100°C temperature range¹⁹⁻²² inside the heat affected zone.

Light absorption and scattering in epithelium

Since melanin is present in the epithelium layer while the hemoglobin is not, and since there is no melanin in hemoglobin-rich connective tissue (sub-epithelium), the optical properties of epithelium and sub-epithelium are analyzed separately and independently from each other.

Similar to melanin content and pigmentation in human epidermis,³ the epithelium's

volume fraction of melanin pigmentation (presented in Figure 4) is estimated at approximately 2% (very light pigmentation), 13% (moderate), and 30% (dark). Optical absorption in epithelium at 800-1,100 nm Near-IR wavelengths is highly dependent on pigmentation but is relatively low due to very thin epithelium (100-300 μm^6).

Unlike Near-IR wavelengths, the Mid-IR wavelengths (Erbium lasers) and IR wavelengths (CO_2 laser) exhibit close to 100% absorption in epithelium, which is of high value for predictable laser photo-thermal ablation of epithelium.¹¹

Light absorption and scattering in sub-epithelium connective tissue

Optical absorption depth spectrum for connective tissue (sub-epithelium) with 75% water and estimated 10% blood presence in the human soft tissue¹² (containing hemoglobin (and/or oxyhemoglobin) at normal concentration of 150g/L^{5,6}) is derived from absorption coefficient spectra (presented in Figure 4) for water^{1,2}, hemoglobin and oxyhemoglobin⁴⁻⁶ and is presented in Figure 7. An estimate of the attenuation depth as an inverse of the sum of absorption coefficient³⁻⁶ and reduced scattering coefficient for whole blood (estimated through absorption to reduced scattering ratio from¹⁴), is presented as inset in Figure 7. Attenuation depth is a more accurate representation of laser energy penetration into the tissue for Near-IR wavelength where light scattering dominates over absorption.^{3-6,14}

As can be seen from Figure 7, both Erbium lasers (approximately 3,000 nm) and CO_2 lasers (approximately 10,000 nm) are highly efficiently absorbed by the soft tissue and, as will be shown, are efficient at cutting and ablating the soft tissue purely radiantly (non-contact). At the same time, diode lasers (approximately 1,000 nm) are highly inefficiently absorbed by the soft tissue, and therefore, cannot be used radiantly (non-contact) for cutting and ablating the soft tissue. Instead, Near-IR diodes are used as hot-tip contact thermal devices, whereas laser radiation heats the charred glass tip and then the heat from the charred tip is conducted into the soft tissue.

Thermal relaxation time

Soft tissue ablation and coagulation efficiencies are influenced not only by absorption/attenuation spectra described in Figures 4 and 7, but also by laser pulse

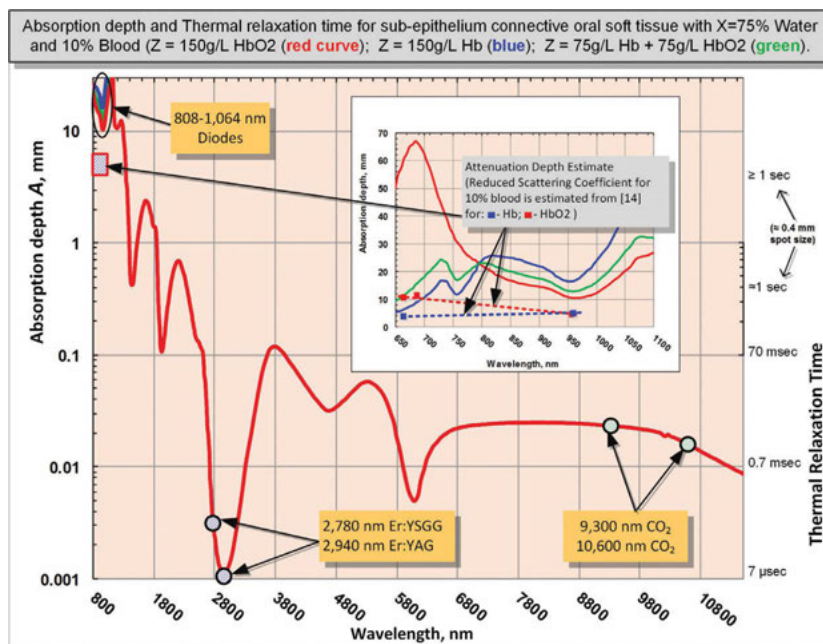


Figure 7: Absorption (and estimated Near-IR attenuation) depth spectra of sub-epithelium (connective tissue). Logarithmic scale is in use

temporal characteristics and tissue' thermal conductivity.

The rate of how fast the irradiated tissue diffuses the heat away is defined through the thermal diffusion time, or Thermal Relaxation Time (presented in Figure 7) as $T_R = A^2/K$,^{16,17} where **A** is optical absorption (or Near-IR attenuation) depth discussed above. The physics behind thermal diffusivity process is similar to diffusion and Brownian motion first described in¹⁵. Coefficient **K** is tissue's thermal diffusivity; $K = \lambda / (\rho C) \approx 0.155 (+/-0.007) \text{ mm}^2/\text{sec}$ (derived from heat conductivity $\lambda \approx 6.2\text{-}6.8 \text{ mW/cm } ^\circ\text{C}$; specific heat capacity $C \approx 4.2 \text{ J/g } ^\circ\text{C}$, and density $\rho \approx 1 \text{ g/cm}^3$ for liquid water for temperatures in 37-100 $^\circ\text{C}$ range²³). For practical consideration of often used 0.4 mm laser beam diameter on the tissue, the Thermal Relaxation Time in Figure 7 is estimated approximately $\geq 1 \text{ sec}$ for absorption (attenuation) depths in excess of 0.4 mm (i.e. when the 2-D radial heat conduction away from the axis of the beam takes place).

Practical implications of Thermal Relaxation Time concept are simple and yet very powerful for appropriate application of laser energy.

The most efficient heating of the irradiated tissue takes place when laser pulse energy is high and its duration is much shorter than T_R . The most efficient cooling of the tissue adjacent to the ablated zone takes place if time duration between laser pulses is much greater than T_R . Short laser pulse, depicted

in Figure 6, allows for the most efficient ablation of the irradiated tissue with minimum coagulation and hemostasis underneath the ablated tissue. For instance, rapidly pulsed Erbium and CO_2 lasers are efficient at cutting with minimal coagulation in applications like char-free stage II implant uncovering, gingivectomy, frenectomy, biopsy, de-epithelization, fibroma excision, etc.

The least efficient heating of the irradiated tissue takes place when laser pulse energy is low, and its duration is much longer than T_R . The least efficient cooling of the tissue adjacent to the ablated zone takes place if time duration between laser pulses is much shorter than T_R . For instance, long pulse and continuous wave (CW) CO_2 lasers are less efficient cutters but provide for greater depth of coagulation for excising/incising in highly vascular and inflamed tissues like hemangioma.

Photo-thermal ablation efficiency

Soft tissue photo-thermal ablation (or photovaporolysis^{5,6}) is a process of vaporization of intra- and extra-cellular water.^{5,6,17} For a fixed laser beam diameter (or spot size), the volume of the tissue exposed to laser beam is proportional to the optical penetration (i.e. absorption or Near-IR attenuation as defined above) depth. The shorter the penetration depth — the less energy is required to ablate the tissue. The longer the optical penetration depth — the greater the volume of irradiated tissue, and therefore, more energy is

required to ablate the tissue within the irradiated volume of tissue.

The minimum energy density requirement to vaporize the irradiated soft tissue can be calculated from the spatial distribution of laser light intensity (**1**) inside the irradiated tissue (see Figure 6) for different wavelengths that are relevant to practical soft tissue dental Near-IR Diode, Mid-IR Erbium and IR CO₂ lasers. Present analysis below covers conditions most suited for high efficiency photo-thermal ablation (pulse duration $t \leq T_R$) with minimum collateral damage to the surrounding tissue (pulse repetition rate $f \ll 1/T_R$).

Consider a laser beam pulse characterized by the following: 1) its duration **t** is less than Thermal Relaxation Time T_R (for the thermal confinement of the laser energy within the irradiated tissue); and 2) its penetration (i.e., absorption or attenuation defined previously) depth **A** is uniquely defined by the laser wavelength and tissue properties; and 3) for the Near-IR wavelengths, the beam diameter is large enough so that its increase due to light scattering is negligible as it propagates through the tissue. Ablation depth is x_a and coagulation depth is $H = x_a - x_c$, where the end of coagulation zone x_c is where the tissue temperature T_c equals 60°C.

Let's consider $x_a \ll A$ conditions for which both the "blow-off" and "steady-state" ablation models described in¹⁷ apply. For laser beam intensity given by formula (1), the laser energy deposited into the unit volume of the tissue (during laser pulse duration **t**) is proportional to the rate of laser beam' intensity's change:

$$t \, dl/dx = -t I_0 \text{Exp}[-x/A] / A = -t I / A \quad (2)$$

Laser energy absorbed by the tissue heats up the tissue. Soft tissue ablation (i.e., tissue's water vaporization) intensity I_a at location $x = x_a$ can be derived from (2) as:

$$\rho (C(T_a - T_b) + r) = t I_a / A = t I_0 \text{Exp}[-x_a/A] / A \quad (3)$$

where T_b is body temperature at 37°C, T_a is water boiling temperature is 100°C, $C=4.2$ J/g °C is specific heat capacity, $r=2,260$ J/g is latent heat of water evaporation [27], and $\rho=1$ g/cm³ is water density. The greater the laser beam pulse energy density $t I_0$, the deeper (i.e. greater x_a) the ablation.

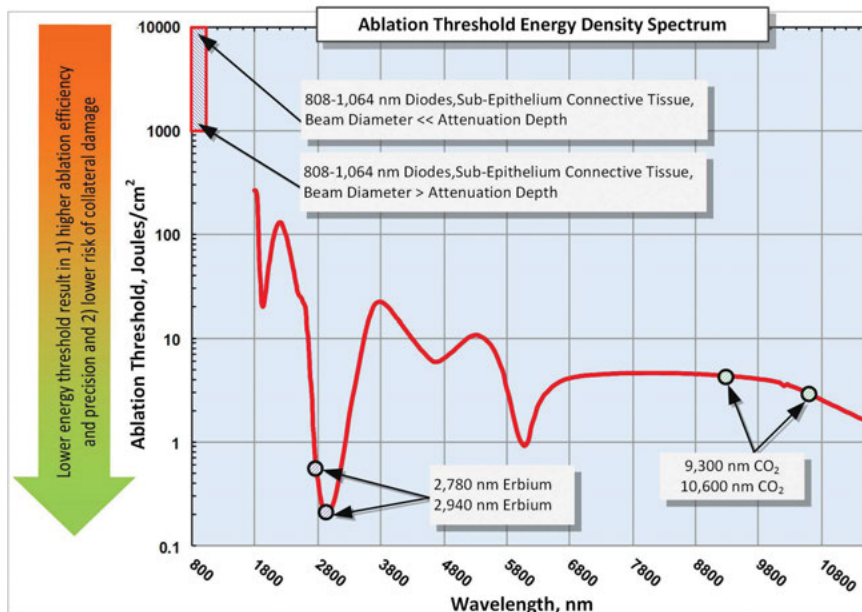


Figure 8: Soft tissue ablation threshold energy density spectrum. Logarithmic scale is in use

The key to the success of soft tissue lasers is their ability to cut and coagulate the soft tissue at the same time.

In order to calculate from (3) the minimum (i.e. threshold) ablation energy density E_{TH} of laser beam, we consider $x_a \ll A$ conditions:

$$E_{TH} = t I_{TH} = \rho A (C(T_a - T_b) + r) \quad (4)$$

The ablation threshold energy density E_{TH} spectrum is presented in Figure 8, where the Near-IR wavelengths 800-1,100 nm are characterized by 100s-1,000s times greater photo-thermal ablation threshold energy densities than Mid-IR and IR wavelengths because of weak Near-IR absorption by the soft tissue's chromophores. For the Near-IR, the ablation threshold energy density is the lowest when the beam diameter is large enough so that its increase (due to scattering) is negligible as it propagates through the tissue. For very small Near-IR beam diameters, the ablation threshold energy density is significantly greater due to radial optical scattering as the beam propagates through the tissue. Figure 3 illustrates the high degree of scattering and predicted absence of tissue ablation at 810 and 980 nm.

In sharp contrast to Near-IR wavelengths, the Mid-IR and IR wavelengths are highly energy efficient at ablating the soft tissue photo-thermally with very low

ablation threshold intensities (see Figure 8) due to extremely small volumes of irradiated tissue because of extremely short absorption depths (see Figure 7).

Spatial accuracy of photo-thermal ablation

Near-IR 800-1,100 nm wavelengths (dental diodes' operating wavelengths) are poorly absorbed by scarce melanin in epithelium and by low concentration hemoglobin and oxyhemoglobin in sub-epithelium connective tissue, which results in multi-millimeter depth of laser energy penetration into the oral soft tissue. Such multi-millimeter ambiguity in tissue removal spatial accuracy at Near-IR wavelengths (also cited in⁵ as "poor scalpels" and in¹⁷ as "not conducive to precise ablation") increases the collateral damage risk of overheating both soft and hard dental structures (enamel, dentin, implants, and bone) underneath the connective soft tissue if photo-thermal ablation is attempted. Such risk is referred to in¹⁸ as "vital structures ... may be heavily damaged before tissue ablation at the surface initiated"; the 810 nm soft tissue absorption coefficient of 0.7 1/cm in¹⁸ makes its observations highly relevant to the present analysis where 10% blood absorbs

at the rate of approximately 0.4 1/cm at 810 nm (see Figure 4).

Unlike Near-IR wavelengths, the Mid-IR wavelengths (Erbium lasers) and IR wavelengths (CO₂ lasers) exhibit much shorter absorption depths (see Figure 7), which makes Mid-IR and IR lasers far more spatially precise and safer in soft tissue ablative applications.

Photo-thermal coagulation efficiency

Coagulation occurs as a denaturation of soft tissue proteins that occurs in 60-100°C temperature range¹⁹⁻²² leading to a significant reduction in bleeding (and oozing of lymphatic liquids) on the margins of ablated tissue during laser ablation (and excision, incision) procedures. Since blood is contained within and transported through the blood vessels, the diameter of blood vessels **B** (estimated to range from 21 to 40 μm with average value of 31 μm – from measurements in human cadaver gingival connective tissue²⁴) is a highly important spatial parameter that influences the efficiency of photocoagulation process. Photo-thermal coagulation is also accompanied by hemostasis due to shrinkage of the walls of blood vessels (and lymphatic vessels) due to collagen shrinkage at increased temperatures.

Present analysis below covers conditions most suited for high efficiency photo-thermal ablation (pulse duration $t \leq T_R$) with minimum collateral damage to the surrounding tissue (pulse repetition rate $f \gg 1/T_R$). Laser light intensity, see Figure 6, is assumed at the ablation threshold I_{TH} from (4), and $x_a \ll A$.

For short laser pulses $t \ll T_R$ and for near-ablation threshold conditions (2)-(4) above, the coagulation threshold power density $E_c = t I_c$ and coagulation depth $H = x_c - x_a \approx x_c$ (for 60-100°C temperature range inside the heat affected zone in Figure 6, i.e. $T_a = 100^\circ\text{C}$ and $T_c = 60^\circ\text{C}$) is calculated from:

$$\rho C (T_c - T_b) = E_c / A = t I_0 \text{Exp} [-x_c/A] / A = E_{TH} \text{Exp} [-H/A] / A \quad (5)$$

where body temperature T_b is 37°C. For longer laser pulses closer to Thermal Relaxation Time ($t \approx T_R$), the thermal diffusion spreads the heat over an additional distance **A**, which accordingly increases the coagulation depth from (5).

The coagulation depth value **H** relative to the blood vessel diameter **B** is an important measure of coagulation and hemostasis

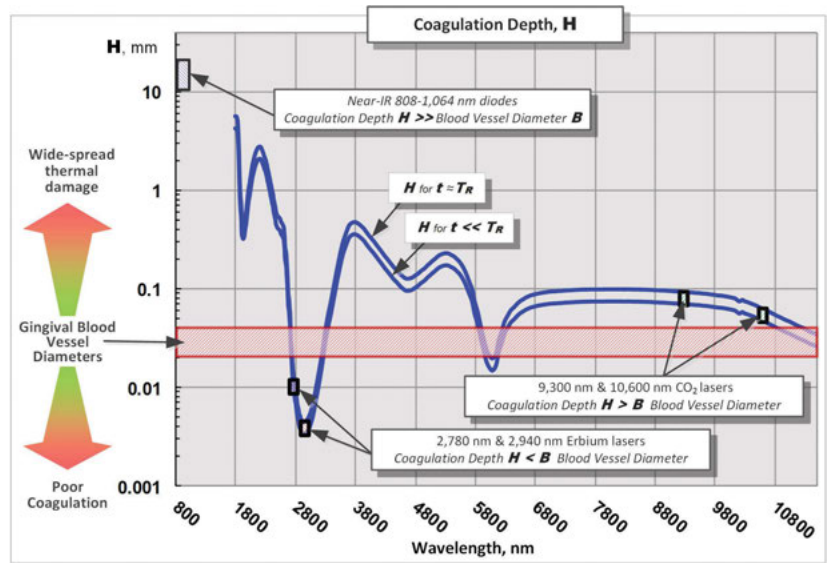


Figure 9: Coagulation depth spectrum for ablation threshold conditions. Logarithmic scale is in use

efficiency; and is presented in Figure 9 for $B = 21-40 \mu\text{m}$ ²⁴, where absorption/attenuation depth **A** from Figure 7 is utilized to calculate **H** from (5).

For $H \ll B$ (see Erbium laser wavelengths in Figure 9), optical absorption and coagulation depths are significantly smaller than blood vessel diameters; coagulation takes place on relatively small spatial scale and cannot prevent bleeding from the blood vessels severed during tissue ablation.

For $H \gg B$ (diode laser wavelengths in Figure 9), optical absorption (Near-IR attenuation), and coagulation depths are significantly greater than blood vessel diameters; coagulation takes place over extended volumes — far away from ablation site where no coagulation is required. Extended thermal damage zones for Near-IR irradiated soft tissue are documented in¹⁸; the 810 nm soft tissue absorption coefficient 0.7 1/cm in¹⁸ makes its observations highly relevant to present analysis with absorption coefficient of approximately 0.4 1/cm at 810 nm (see Figure 4).

For $H \geq B$ (CO₂ laser wavelengths in Figure 9), coagulation extends just deep enough into a severed blood vessel to stop the bleeding; the coagulation is more efficient then for the above two cases $H \ll B$, and $H \gg B$.

Near-IR diode and Nd:YAG laser soft tissue ablation and coagulation

Near-IR diode laser light circa 1,000 nm is not used to optically ablate the oral soft tissue; instead, the diode laser optical energy is used to heat up the charred distal end of the fiber glass tip to 500-900°C,²⁸ which

then heats up the soft tissue through heat conduction from hot glass tip: soft tissue is burned off (ablated) on contact with the hot charred glass tip, while the margins of the burn are coagulated. Unlike non-contact surgical lasers (such as CO₂ or Erbium), the soft tissue ablative diodes are contact thermal non-laser wavelength-independent devices.

When used in contact mode, the Nd:YAG laser may function as a hot tip cutting tool [6]. When used in non-contact mode, the Nd:YAG laser's 1,064 nm wavelength is a highly efficient coagulator, but a poor scalpel, as it is highly scattered and weakly absorbed by the soft tissue.^{5,6,17} The low absorption of the Nd:YAG wavelength may be attenuated (and, therefore, its cutting efficiency may be enhanced) by the use of very high peak power⁶ typical for free-running pulsed Nd:YAG lasers.

Summary and conclusions

Ablation threshold intensity and coagulation depth spectra are derived from the absorption spectra of oral soft tissue' main chromophores (water, melanin, hemoglobin, and oxyhemoglobin) for conditions most suited for high efficiency photo-thermal ablation (pulse duration $t \leq T_R$) with minimum collateral damage to the surrounding tissue (pulse repetition rate $f \ll 1/T_R$). The non-laser wavelength-independent thermal interaction between the soft tissue and diode's charred hot glass tip was excluded from the scope of present analysis.

Near-IR 800-1,100 nm diode wavelengths are shown to be highly energy

inefficient and spatially inaccurate photo-thermal ablation tools with wide spread thermal damage. More measurement data on Near-IR reduced scattering coefficient are needed for more accurate calculations of the oral soft tissue photo-thermal ablation and coagulation properties in the Near-IR.

Mid-IR Erbium laser wavelengths are shown to be highly energy efficient and spatially accurate photo-thermal ablation tool with poor coagulation efficiency. Coagulation depth can be increased by pulse width/rate increase.

IR CO₂ laser wavelengths are shown to be highly efficient and spatially accurate photo-thermal ablation tool with excellent coagulation efficiency (close match between coagulation depth and oral soft tissue blood capillary diameters). Coagulation depth can be increased by pulse width/rate increase. **IP**

REFERENCES

1. Wieliczka DM, Weng S, Querry MR. Wedge shaped cell for highly absorbent liquids: infrared optical constants of water. *Appl Opt.* 1989;28(9):1714-1719.
2. Hale GM, Querry MR. Optical constants of water in the 200-nm to 200-microm wavelength region. *Appl Opt.* 1973;12(3):555-563.
3. Jacques SL. Origins of tissue optical properties in the UVA, visible, and NIR regions. In: Alfano RR, Fujimoto JG, ed. *OSA TOPS on Advances in Optical Imaging Photon Migration, Volume 2.* Optical Society of America; 1996:364-369.

4. Jacques SL. Optical properties of biological tissues: a review. *Phys Med Biol.* 2013;58(11):R37-R61.
5. Fisher JC. Basic laser physics and interaction of laser light with soft tissue. In: Shapshay SM, ed. *Endoscopic Laser Surgery Handbook.* New York, NY: Marcel Dekker; 1987:96-125.
6. Fisher JC. Qualitative and quantitative tissue effects of light from important surgical lasers. In: Wright CV, Fisher JC, eds. *Laser Surgery in Gynecology: A Clinical Guide.* Philadelphia, PA: Elsevier Health Sciences; 1993:58-81.
7. Convisar RA. *Principles and Practice of Laser Dentistry.* St. Louis, MO: Mosby Elsevier; 2011.
8. Prestin S, Rothschild SI, Betz CS, Kraft M. Measurement of epithelial thickness within the oral cavity using optical coherence tomography. *Head Neck.* 2012;34(12):1777-1781.
9. Squier CA, Brogden KA, eds. *Human Oral Mucosa: Development, Structure, and Function.* Chichester, West Sussex, UK: Wiley-Blackwell; 2011:14-16.
10. Squier CA, Finkelstein MW. Oral mucosa. In: Nanci A, ed. *Ten Cate's Oral Histology: Development, Structure, and Function.* 7th ed. St. Louis, MO: Mosby Elsevier; 2007:319-57.
11. Esen E, Haytac MC, Oz IA, Erdoğan O, Karsli ED. Gingival melanin pigmentation and its treatment with the CO₂ laser. *Oral Surg Oral Med Oral Pathol Oral Radiol Endod.* 2004;98(5):522-527.
12. Alberts B, Johnson A, Lewis J, Raff M, Roberts K, Walter P. *Molecular Biology of the Cell.* 5th ed. New York, NY: Garland Science; 2007:Table 23-1.
13. Collier T, Arifler D, Malpica A, Follen M, Richards-Kortum R. Determination of epithelial tissue scattering coefficient using confocal microscopy. *IEEE J of Quant Electronics.* 2003;9(2):307-313.
14. Cheong WF, Prahl SA, Welch AJ. A review of the optical properties of biological tissues. *IEEE J of Quant Electronics.* 1990;26(12):2166-2185.
15. Einstein A. Über die von der molekularkinetischen Theorie der Wärme geforderte Bewegung von in ruhenden Flüssigkeiten suspendierten Teilchen. *Annalen der Physik.* 1905;322(8):549-560.
16. Svaasand LO. Lasers for biomedical applications. In: Driggers RG, Hoffman C, eds. *Encyclopedia of Optical Engineering.* New York, NY: CRC Press; 2003:1035-1041.
17. Vogel A, Venugopalan V. Mechanisms of pulsed laser ablation of biological tissues. *Chem Rev.* 2003;103(2):577-644.

18. Willems PW, Vandertop WP, Verdaasdonk RM, van Swol CF, Jansen GH. Contact laser-assisted neuroendoscopy can be performed safely by using pretreated 'black' fibre tips: experimental data. *Lasers Surg and Med.* 2001;28(4):324-329.
19. Pfefer TJ, Choi B, Vargas G, McNally KM, Welch AJ. Mechanisms of Laser-Induced Thermal Coagulation of Whole Blood In Vitro. Part of the SPIE Conference on Cutaneous Applications of Lasers: Dermatology, Plastic Surgery, and Tissue Welding. *Proc SPIE.* 1999;3590:20-31.
20. Barton JK, Rollins A, Yazdanfar S, Pfefer TJ, Westphal V, Izatt JA. Photothermal coagulation of blood vessels: a comparison of high-speed optical coherence tomography and numerical modelling. *Phys Med Biol.* 2001;46(6):1665-1678.
21. Mordon S, Rochon P, Dhelin G, Lesage JC. Dynamics of temperature dependent modifications of blood in the near-infrared. *Lasers Surg Med.* 2005;37(4):301-307.
22. Pang P, Andreana S, Aoki A, Coluzzi D, Obeidi A, Olivi G, Parker S, Rechmann P, Sulewski J, Sweeney C, Swick M, Yung F. Laser energy in oral soft tissue applications. *J Laser Dent.* 2010;18(3):123-131.
23. Weast RC, ed. *CRC Handbook of Chemistry and Physics.* 61st ed. Boca Raton, FL: CRC Press; 1980-1981.
24. Yoshida S, Noguchi K, Imura K, Miwa Y, Sunohara M, Sato I. A morphological study of the blood vessels associated with periodontal probing depth in human gingival tissue. *Okajimas Folia Anat Jpn.* 2011;88(3):103-109.
25. Graeber J. Diode Lasers: A Primer. The Academy of Dental Therapeutics and Stomatology – Your Online Continuing Education Resource. IneedCE.com. http://www.ineedce.com/coursereview.aspx?url=2564%2FPDF%2F1401ce1Graeber_rev3.pdf&scid=15269. Published January 2014. Accessed September 2014.
26. Coluzzi D. Fundamentals of lasers in dentistry, basic science, tissue interaction, and instrumentation. *J Laser Dent.* 2008;16(spec issue):4-10.
27. Latent Heat. Encyclopedia Britannica. <http://www.britannica.com/EBchecked/topic/331406/latent-heat>. Accessed August 10, 2014.
28. Romanos G. Diode Laser Soft-Tissue Surgery. *Compend Contin Educ Dent.* 2013;24(10):752-758. <http://editiondigital.net/publication/?i=183287&p=38>. Accessed August 2 2014.

Stage II IMPLANT UNCOVERING with LightScalpel angled tipless handpiece

www.LightScalpel.com

1. Healed implant site ready for uncovering



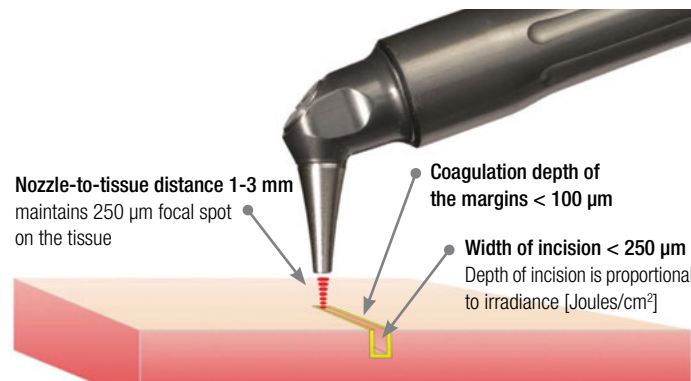
2. Tissue ablation begins in the center above the implant and continues in a circular spiraling motion



3. Implant uncovered after ablation



Incision/excision/ablation with focused laser beam



Coagulation with defocused laser beam

